Climatic warming disrupts recurrent Alpine insect outbreaks

Derek M. Johnson[a,1], Ulf Büntgen[b,c], David C. Frank[b,c], Kyrre Kausrud[d], Kyle J. Haynes[e], Andrew M. Liebhold[f], Jan Esper[g], and Nils Chr. Stenseth[d]

[a]Department of Biology, University of Louisiana, Lafayette, LA 70504; [b]Dendro Science Unit, Swiss Federal Research Institute WSL, 8903 Birmensdorf, Switzerland; [c]Oeschger Centre for Climate Change Research, University of Bern, 3012 Bern, Switzerland; [d]Department of Biology, Centre for Ecological and Evolutionary Synthesis (CEES), University of Oslo, N-0316 Oslo, Norway; [e]The Blandy Experimental Farm, University of Virginia, Boyce, VA 22620; [f]Northern Research Station, US Department of Agriculture Forest Service, Morgantown, WV 26505; and [g]Department of Geography, Johannes Gutenberg University, 55099 Mainz, Germany

Edited* by Gordon H. Orians, University of Washington, Seattle, WA, and approved October 20, 2010 (received for review July 15, 2010)

Climate change has been identified as a causal factor for diverse ecological changes worldwide. Warming trends over the last couple of decades have coincided with the collapse of long-term population cycles in a broad range of taxa, although causal mechanisms are not well-understood. Larch budmoth (LBM) population dynamics across the European Alps, a classic example of regular outbreaks, inexplicably changed sometime during the 1980s after 1,200 y of nearly uninterrupted periodic outbreak cycles. Herein, analysis of perhaps the most extensive spatiotemporal dataset of population dynamics and reconstructed Alpine-wide LBM defoliation records reveals elevational shifts in LBM outbreak epicenters that coincide with temperature fluctuations over two centuries. A population model supports the hypothesis that temperature-mediated shifting of the optimal elevation for LBM population growth is the mechanism for elevational epicenter changes. Increases in the optimal elevation for population growth over the warming period of the last century to near the distributional limit of host larch likely dampened population cycles, thereby causing the collapse of a millennium-long outbreak cycle. The threshold-like change in LBM outbreak pattern highlights how interacting species with differential response rates to climate change can result in dramatic ecological changes.

traveling wave | tree rings | tri-trophic | Lepidoptera | parasitoids

Climate change affects biotic systems in a number of ways, including elevational species range shifts (1), changes in phenology (2), extinction (3), and altered results of biotic interactions such as with competitors and natural enemies (4, 5). Global warming has recently been implicated in elevational range shifts of plants (1, 6) and animals (7, 8) at various spatiotemporal scales (9). Range shifts are often slow and may lag behind climate changes, and thus, effects of recent warming may not yet be observable (10). Patterns of population dynamics within an established range, however, should respond more quickly to external forcing, sometimes within several generations. Over the last few decades, regional scale warming trends have coincided with the collapse of population cycles across a broad range of taxa, leading to the hypothesis that such collapses are the result of climatic forcing (11, 12). However, a mechanistic understanding of cycle collapses has proven to be challenging because of limited long-term data on cyclical populations. Most such records are restricted to only a few population cycles—too few to robustly confirm changes in dynamical behavior and attribute them to causal factors.

Larch budmoth [LBM; *Zeiraphera diniana* Gn. (Lepidoptera: Torticidae)] population dynamics are a classic example of regular population cycles (13), because outbreaks have occurred periodically, almost without fail, every 8–10 y since A.D. 800 (14). The oscillations span a remarkable five orders of magnitude between population density peaks and troughs (13). Spatiotemporal patterns of 20th century LBM outbreaks indicate recurring traveling waves of defoliation that spread from a western epicenter in an eastward direction across the Alpine arc (15, 16). Inexplicably, however, the regular outbreaks and the accompanying defoliation of European larch forests (*Larix decidua* Mill.) have largely vanished since the early 1980s (14).

The 20th century warming trend has been shown to result in an increase in the elevation at which plant species abundances peak in western Europe (1), and this likely has similar effects on a broad range of taxa (10). The optimal elevational zone for larch defoliation by the LBM in the late 20th century was estimated to be 1,700–2,000 m above sea level (asl) near the larch timberline, as evidenced by both the highest frequency and earliest occurrence of LBM outbreaks within cycles (17). In contrast, outbreaks between 1,200 and 1,600 m asl were less frequent and lagged by ∼1–4 y, resulting in a temporal gradient in outbreak across a mountain slope. Thus, the spatial pattern of LBM outbreaks should reveal elevational shifts in response to temperature fluctuations over the last two centuries. Sufficient warming may force LBM outbreak activity to the larch timberline in the Alps. Because there is a considerable time lag between climatic shifts and elevational changes in timberline, this would result in a reduction or cessation of the LBM outbreak phenomenon, because the resource biomass is greatly reduced as the timberline is approached.

Forest insect outbreaks often leave distinct and quantifiable signals in tree rings because defoliation significantly reduces radial growth and wood density during and after an outbreak year (14, 17–19). These living templates, thus, provide historical information that extends back in time for centuries, long enough to detect climatic effects on ecological systems. The effectiveness of reconstructing LBM outbreaks from larch tree rings has been confirmed over exceptional temporal (14) and spatial scales (18). Although ring width and density data provide evidence for a link between LBM outbreaks and temperature fluctuations over the last two centuries (20, 21), a causal mechanism remains unresolved (18). Herein, we quantified changes in the elevational pattern of LBM outbreaks over the last two centuries and applied a simulation model to provide insight into the mechanisms of climatic forcing and the cessation of LBM outbreaks.

We hypothesize that temperature-mediated shifts in the elevation of optimal LBM growth rates cause elevational shifts in LBM outbreak epicenters. Gradients in population growth rate, a reasonable proxy for habitat quality, have proven capable of generating traveling waves originating in optimal habitat (16). A traveling wave is characterized by temporal lags in spatial synchrony where peaks in population density move across a spatial gradient over time (16). We used wavelet-phase angles to test for elevational traveling waves in LBM outbreak cycles that were reconstructed

Author contributions: D.M.J., U.B., D.C.F., K.K., A.M.L., J.E., and N.C.S. designed research; U.B., D.C.F., and J.E. performed research; D.M.J., K.J.H., and A.M.L. analyzed data; and D.M.J. wrote the paper.

The authors declare no conflict of interest.

*This Direct Submission article had a prearranged editor.

[1]To whom correspondence should be addressed. E-mail: derekjohnson@louisiana.edu.

This article contains supporting information online at www.pnas.org/lookup/suppl/doi:10.1073/pnas.1010270107/-/DCSupplemental.

over two centuries using a collection of 3,113 larch tree-ring width series and 150 maximum latewood density series from 65 locations across the Alpine arc (Fig. 1). Wavelet analysis, a spectral analysis, was used to identify the dominant periodicity in LBM outbreaks (circa 8–9 y). Each time series was then subjected to wavelet decomposition at the 8-y scale and converted to mean relative phase angles, which range from −180° to 180°. Mean relative phase angles represent the phase of the cycle at each location relative to the phase angle of the time series averaged over all locations. When comparing locations across elevations, the greatest relative phase angle indicates that LBM outbreak occurred in that elevation before the others (i.e., an epicenter). This unique dataset covers approximately the entire elevational range of larch forest that is susceptible to LBM outbreaks (800–2,300 m asl) and robustly spans two centuries (A.D.1800–2000). The empirical analysis was complemented with a simulation model analysis to test our conceptual model for the mechanism of LBM outbreak collapse.

System

European larch, *L. decidua*, is a deciduous conifer with a lifespan of up to 400 y (22). Similar to most high-elevation trees (23), vertical growth in *L. decidua* declines as elevations approach the climatic timberline, from 20 to 8 cm/y at 1,680 and 1,940 m asl, respectively. Needle biomass, the food source of LBM, is reduced by 80% at 1,940 m compared with 1,680 m asl (24). European larch recruitment requires exposed mineral soil such as results from landslides or cattle disturbance (25). Thus, an upward shift in larch timberline is slow and lags behind climate change because of depressed growth rates, low seed production, short distance dispersal of seeds, and limited regeneration opportunities. In contrast, tree-ring width and density respond to elevation only near the timberline (24) and instead, are mediated by year to year variation in environmental conditions (e.g., LBM defoliation events) (14).

The LBM has a univoltine life cycle. Larvae hatch in the spring and feed on the new flush of needles on deciduous larch hosts. Synchrony between larval hatching and the emergence of needles is critical to survival of first instars (21). The first three instars feed between larch needles, late third and fourth instars create tubular cases by spinning needles together, and fifth instars move freely among branches. In the summer, fifth instar larvae descend to the forest floor to pupate in mineral and leaf litter (26). Adults eclose in the fall, at which time they mate, disperse, lay eggs, and die before winter (13); thus, generations are nonoverlapping.

The two predominant processes thought to drive LBM population cycles are (*i*) host–plant quality interactions and (*ii*) host–parasitoid interactions. The nutritional quality of larch needles declines significantly after a defoliation event and requires 2 or more y to recover. Specifically, in the year after a defoliation event, needle lengths decrease to <20 mm from predefoliation lengths of >30 mm, raw fiber content increases 50%, and protein content decreases 33%. Poor foliage quality has been shown to have a strongly negative effect on LBM larval survival and female fecundity (27, 28). A model of LBM–plant quality dynamics is capable of matching observed periodicity and magnitude of LBM cycles (29).

Mortality rates caused by parasitoids attacking LBM can reach levels as high as 90% (26). Of the more than 100 parasitoid species associated with LBM, only a small subset significantly affects LBM population dynamics. This group consists of three eulophids (*Sympiesis punctifrons*, *Dicladocerus westwoodii*, and *Elachertus argissa*) that primarily attack the third instar and an ichneumonid (*Phytodietus griseanae*) that primarily attacks the fifth instar (26). Based on the observation that peaks in parasitism rates lagged 1–2 y behind peaks in LBM outbreak, Delucchi (26) concluded that parasitoids were merely tracking LBM populations and not regulating them. However, a lag in dynamics is consistent with parasitoid-driven cycles (29, 30). Turchin (31) used both an LBM–parasitoid model and a tritrophic (LBM–parasitoid–plant quality) model to show that parasitoids, in concert with plant quality, likely play a key role in driving LBM cycles (29).

Model

Given the evidence for the roles of both plant quality and parasitoids as potential drivers of LBM cycles, we used the tritrophic model by Turchin (31) of LBM population dynamics to assess whether elevational shifts in a habitat-quality gradient could cause the observed changes in outbreak epicenter during the 20th century. The model (Eqs. **1**–**3**),

$$N'_{i,t+1} = N_{i,t}\exp\left\{(r_{0,i}+u)\left(1-\exp\left[\frac{-Q_{i,t}}{\delta}\right]\right) - \frac{(r_{0,i}+u)N_{i,t}}{k} - \frac{aP_{i,t}}{1+awP_{i,t}}\right\} \quad [1]$$

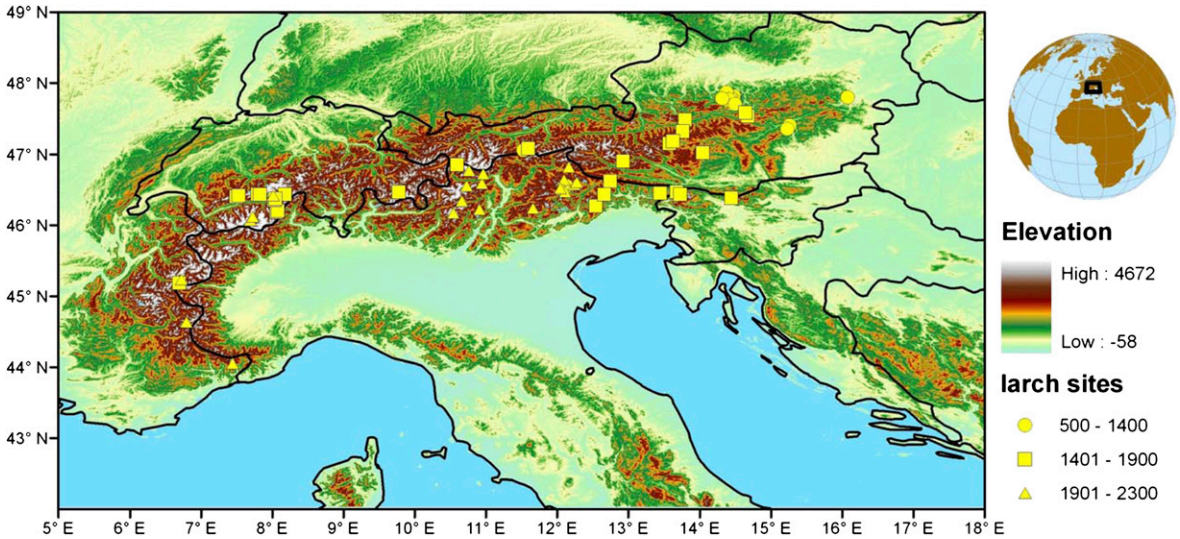

Fig. 1. Location of the 65 larch (*L. decidua* Mill.) tree-ring sites across the European Alps.

$$P'_{i,t+1} = N_t\left\{1 - \exp\left[\frac{-aP_{i,t}}{1 + awP_{i,t}}\right]\right\} \quad [2]$$

$$Q_{i,t+1} = (1-\beta) + \beta Q_{i,t} - \frac{cN_{i,t}}{d + N_{i,t}}, \quad [3]$$

is a discrete-space discrete-time model where the predispersal population dynamics of the LBM (N') are coupled with predispersal population dynamics of parasitoid density (P') and the quality of host foliage (Q), with i and t representing patch and time, respectively. Population density of LBM is modeled as a logistic growth function with environmental stochasticity (u), carrying capacity (k), patch quality (Q) effects, and mortality caused by parasitoid attack. The parameter δ determines the rate at which population growth increases in response to patch quality. Parasitism is modeled as a type II functional response. The population dynamics of parasitoids are a modified form of the classic Nicholson–Bailey host–parasitoid model (32), where a is the prey saturation parameter and w is the parasitoid mutual interference parameter. Patch quality is reduced by LBM herbivory at a rate determined by larval density (N), with the maximum potential reduction determined by c and the one-half maximum reduction parameter d (more generally called a half saturation parameter). Recovery rate of patch quality is determined by the expression $(1 - \beta)$. Elevation-specific intrinsic rate of increase ($r_{0,i}$) was used as a proxy for the underlying elevation–habitat quality relationship. Empirical LBM larval counts at 13 sites were used to estimate the relationship between r_0 and elevation. In a cyclical system, population growth rate is dependent on the phase of the cycle. Thus, to estimate r_0 from empirical LBM larval counts, we best fit phase-specific population growth rates from model simulations to those from the cyclical LBM larval counts by minimizing sums of squares of differences between the standardized $(\bar{x} = 0; \sigma = 1)$ empirical and simulated larval counts. The parameter values ($u = 0.40$, $\delta = 0.22$, $k = 250$, $a = 2.5$, $w = 0.17$, $\beta = 0.55$, $c = 0.90$, and $d = 100$) were empirically estimated in a previous study (31).

The tritrophic model was simulated on a 1D landscape with an elevational gradient from 400 to 2,200 m asl and a patch at every 10 m in elevation (181 patches). We represent redistribution of moths and parasitoids across the elevational gradient with the connectivity parameter (Eq. **4**)

$$\Omega_i = \frac{\sum_{j=1}^{n} e^{-\left(x_{ij}\alpha^{-1}\right)^2}}{C}, \quad [4]$$

which is measured with a Gaussian distribution function. The function sums immigration from all patches j to patches i (when $i \neq j$) and the local contribution (when $i = j$). Elevational distance between patches is represented by x_{ij}. The dispersal parameter α is set higher for the LBM than the parasitoids (40- and 10-m elevation per season, respectively), because the LBM is thought to be capable of dispersing over longer distances (13, 33). The parameter C is a normalization constant that sets $\Omega = 1$ for the most connected patch. Simulated elevational change in the r_0 gradient was modeled as a linear 200-m elevational shift for each 1 °C change in mean seasonal temperature (34).

Results and Discussion

Results from a general linear model analysis strongly imply an effect of elevation on phase angle ($P < 0.001$) and are evidence for elevational traveling waves. An interaction effect between elevation and time interval ($P = 0.049$) implies a temporal shift in the spatial dynamic between A.D. 1800 and 1980 (*SI Text*, *Empirical Evidence for Elevational Traveling Waves and a Temporal Effect* has more details of the methodology). Traveling waves moved from lower to higher elevations over the relatively cool period A.D. 1800–1860 ($P = 0.004$) (Fig. 2*A*). The linear directionality disappeared as temperatures rose out of the little Ice Age between A.D. 1860 and 1920 and during the continued warming period of the 20th century from A.D. 1920 to 1980 (Fig. 2*A*). A more detailed temporal analysis that focused on elevational shifts in the outbreak epicenter implies a strong relationship between changes in mean winter temperature (December, January, and February) (35) and changes in elevation of the outbreak epicenters in the

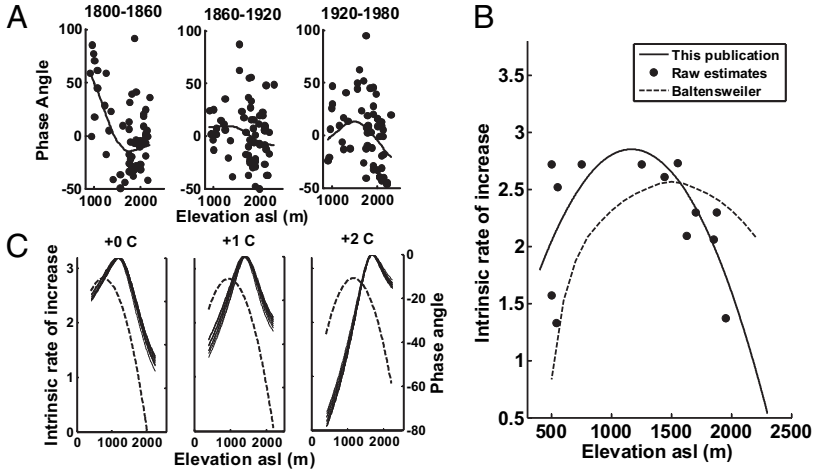

Fig. 2. (*A*) Relationships between elevation and relative phase angle in the three 60-y time intervals from 1800 to 1980. Note a shift from a monotonic negative relationship (indicating traveling waves moving up in elevation) to a unimodal relationship between 1920 and 1980 (indicating a mid-elevation epicenter). (*B*) Relationship between elevation and estimated population growth rate at 13 sites across the Alps. The solid line is an estimate from fitting a quadratic curve to the raw data ($r = x1 \times elev^2 + x_2 \times elev + x_3$), where elevation (*elev*) is measured in meters asl. The estimates and 95% confidence intervals (CIs) for the parameters are $x1 = -1.80 \times 10^{-6}$ [-3.43×10^{-6}, -1.50×10^{-7}], $x_2 = 4.2 \times 10^{-3}$ [2.9×10^{-4}, 8.0×10^{-3}], and $x_3 = 0.40$ [−1.47, 2.27]. The dashed line is an estimate from a previous study (13). (*C*) Model simulations were run with a standardized mean temperature increased by one of three values (+0 °C, +1 °C, and +2 °C). The dashed line indicates the population growth rate–elevation relationship. The clustered solid lines represent the phase angle–elevation relationships in 10 replicate runs.

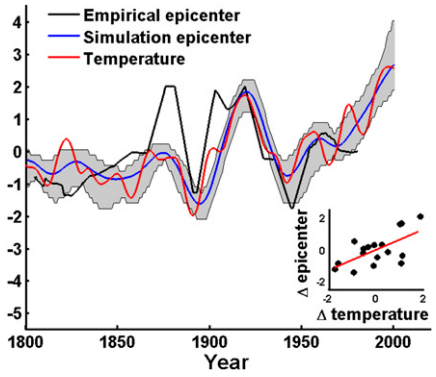

Fig. 3. Mean winter annual temperature (red) and yearly elevation of epicenter (black) in the Alps between A.D. 1800 and 2000. Time series are smoothed using an 8-y average. The blue line is the predicted mean epicenter elevation from 100 simulations given the temperature-specific LBM growth rates and the observed fluctuations in temperature (gray area is the 99% confidence range). *Inset* reveals a positive relationship between standardized temperature and epicenter change over 8-y intervals ($\rho = 0.63$, $P = 0.007$; $n = 17$).

Alps ($\rho = 0.63, P = 0.007; n = 17$) (Fig. 3), particularly after A.D. 1870 when the recent warming trend started (36, 37). No effect of spring, summer, or fall mean temperature on epicenter elevation was found (spring: $\rho = 0.13, P = 0.62$; summer: $\rho = 0.23, P = 0.38$; fall: $\rho = 0.12, P = 0.64; n = 17$). Our results imply that the trend of long-term increase in epicenter elevation is a response to winter warming.

Analysis of LBM larval density time series from across a range of elevations revealed a unimodal relationship between the intrinsic rate of increase (r_0) and elevation (Fig. 2*B*), with a peak in r_0 at 1,100 m asl. A previous study (13), which used a different method to analyze the same dataset, found a similar unimodal relationship but with a higher optimal elevation of 1,700–2,000 m asl. The difference was within the range of estimation error.

Spatial outbreak dynamics of the LBM were simulated between A.D. 1800 and 1980, with the empirically estimated relationship between r_0 and elevation (Fig. 2*B*) and shifts in this relationship mediated by empirical fluctuations in the mean seasonal temperature for each of the four seasons. Correlation analyses between the empirical epicenter elevation time series and the four simulated epicenter elevation time series supported the hypothesis that winter temperature is a better predictor of epicenter elevation (winter: $\rho = 0.36, P = 0.09$; spring: $\rho = 0.20, P = 0.44$; summer: $\rho = 0.02, P = 0.95$; fall: $\rho = -0.15, P = 0.54$; $n = 17$). In a simulation of the tritrophic model, higher winter temperatures caused an upward elevational shift in maximum population growth rate, which resulted in corresponding elevational shifts in outbreak epicenter (Fig. 2*C*). Sensitivity analyses revealed that the simulation results, upward elevation shifts in outbreak epicenters during periods of winter warming, are qualitatively robust across a realistic range of the model parameter values (analyses in *SI Text*, *Sensitivity Analysis*).

In contrast to a recent study, which concluded that LBM outbreak dynamics are regulated by summer temperatures (38), our results strongly suggest that fluctuations in Alpine winter temperature are the main driver of elevational shifts in LBM outbreak epicenters. This is consistent with the findings that increased late winter and early spring temperatures effectively reduce LBM population growth rate by increasing LBM egg mortality and creating a phenological mismatch between larval hatching and spring flush of larch leaves (21, 39).

Although warming can also result in upward shifts in timberlines and enhanced tree growth at higher elevations (40, 41), the response is much slower than any possible LBM range expansion (4). In our models with a moderate amount of advective dispersal and no tree response to climatic warming, an epicenter shift to near and beyond the existing larch timberline resulted in a nonlinear dampening of cycles over a temperature increase of 2–3 °C (Fig. 4). Specifically, as the mean temperature increased, the population densities at the cycle peaks declined to potentially below outbreak densities in a threshold-like response. The cycles continue but possibly below outbreak levels. Thus, the model results support the hypothesis that warming winter temperatures are a causal factor in the near cessation of LBM outbreaks across the Alps since the early 1980s.

The epicenter shift is concurrent with the recent disappearance of larch budmoth outbreaks (14), and our analysis provides evidence for understanding a shared causal mechanism—increased egg mortality under exposure to higher temperatures (39). Investigating the effects of environmental factors other than temperature was beyond the scope of this study, but elevational gradients in precipitation, oxygen, nutrient availability, and other environmental factors may play a role in timberline dynamics (23) and response of LBM outbreak dynamics to climate change.

Other phenological effects, such as timing of LBM activity relative to resource availability and/or natural enemies, may also be at play in this complex ecological system (21). Because larch is deciduous, it is particularly important to moth survival that larval hatching is synchronized with the spring flush of foliage. A warming of 1 °C translates into a 7-d shift in the onset of the larch growing season in the Swiss Alps (42). A mistimed shift in LBM hatching could result in no available food (early hatching) or needles that have toughened too much to be edible by first instars (late hatching). Although coniferous hosts exhibit a degree of seasonality in growth of new tender foliage, early larval hatches may be able to survive on the suboptimal older growth until the spring flush. These results imply that climate change may have a greater effect on insects on deciduous hosts than on coniferous hosts.

In this study, we showed how climatic warming affects the elevational population dynamics of a periodically cycling insect. The key insight is that, in a climatic warming scenario, differing response rates between an herbivore and its host can create a mismatch in ranges and phenology of the two species and result in regimen shifts in population dynamics. The effect will be particularly apparent when a highly mobile herbivore feeds on a host with a long generation time, such as a high-elevation tree species (e.g., the LBM–larch system). We suggest that similar shifts in population dynamical regimens may be occurring across a broad range of systems, but the patterns and mechanism are often obscured by inherent stochastic noise in the systems and require large spatiotemporal datasets to detect.

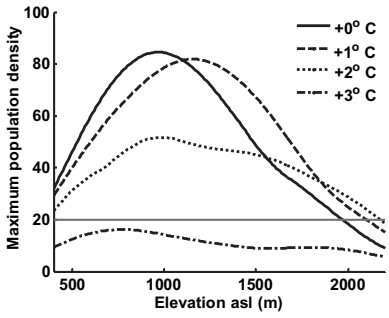

Fig. 4. The effect of increasing temperature on maximum population density across an elevational gradient. The coolest scenario (black solid line) approximates the mean temperature in the Alps in the 1800s. Each additional scenario represents a 1 °C increase in temperature. The 2 °C increase, approximating the 1800–1980 increase, resulted in a significant reduction in maximum outbreak intensity. An additional warming of 1 °C resulted in population damping to below a hypothetical outbreak threshold (horizontal gray line).

Conclusion

The A.D. 2007 winter surface air temperature in the greater Alpine region was probably the warmest in over 500 y (43), and temperature anomalies are predicted to increase as much as 5 SD by the end of the 21st century (44). Winter warming over the next century is projected to be most pronounced at high latitudinal and altitudinal land regions (45). Our analysis reveals that LBM outbreak dynamics are strongly driven by winter temperatures; thus, the dynamics of LBM are likely to be highly sensitive to climate change. Forest insect outbreaks are generally more common in higher latitudes and thus, are likely to be greatly affected by global warming. Ecological responses to global warming, which include range shifts to higher latitudes and elevations, have already been observed in a broad range of taxa. Range-restricted species in polar and montane habitats are in particular danger of extinction because of vanishing habitat in a warmer world (4).

Insect outbreaks have been predicted by some to increase in frequency and intensity under predicted global climate change because of (possibly transient) disruption of coevolved species interactions (5, 46). Conversely, recurrent outbreak cycles are disappearing in a subset of species for which such cycles are the historical normal, although the driving mechanisms are largely unknown and likely vary among species (11). Warming rates may reduce outbreaks in the LBM while catalyzing outbreaks in other species. It should be no surprise that the effects of climate change are system-specific. The results herein highlight how differential response rates to climate change among interacting species can result in dramatic and sometimes unpredictable ecological changes. One overriding pattern is that climate change is and will continue to alter population dynamics over a broad range of taxa.

Methods

Tree-Ring Network Analysis. Tree-ring width and density measurements from >3,000 European larch (*L. decidua* Mill.) series from 65 sites across the Alpine arc were recorded. This unique network includes living and relict samples and was initially introduced by Buntgen et al. (18). Sufficient site replication and spatial coverage are limited to the A.D. 1800–2000 period. High-resolution 0.5° × 0.5° grids of monthly temperature means and precipitation totals were used for growth/climate response analysis and subsequent LBM detection (35, 47). Six methods were used to separate LBM fingerprints from other disturbance factors (*SI Text*, *Analysis of Tree-Ring Network* has greater detail on tree-ring analysis methodology).

Wavelet-Phase Analysis. We used wavelet-phase analysis to characterize spatial waves in LBM outbreaks between A.D. 1800 and 1980. The Morlet wavelet function (a damped complex exponential) was adequate for characterizing periodicities in the LBM outbreak data (*SI Text*, *Wavelet-Phase Analysis* has details about the method). For the purpose of this analysis, outbreak epicenters are characterized by having the largest phase angle. Traveling waves expanding from the epicenter move across a gradient of locations with progressively smaller phase angles. The phase-angle data were detrended (i.e., the large-scale west–east wave of outbreak was removed) by fitting the phase-angle data to a cubic smoothing spline along the longitudinal gradient. The resulting phase-angle residuals were analyzed for an elevational effect. The last 20 y (A.D. 1980–2000) were omitted from the analysis, because outbreaks were lacking during this period.

Epicenter Temperature Analysis. The empirical time series of temporal fluctuations in the epicenter elevation, estimated from the tree-ring network, were compared with reconstructions of mean seasonal temperature across the Alpine arc between A.D. 1800 and 2000 (35). The empirical epicenter elevation is reported as a 10-y moving average, approximately equal to the outbreak periodicity in the system. The four temperature time series were smoothed with 20-y splines from winter (December, January, and February), spring (March, April, and May), summer (June, July, and August), and fall (September, October, and November). It is reasonable for the predictor variable (temperature) to be based on a longer smoothing function (20-y spline) than the response variable (epicenter elevation is a 10-y average), because the momentum inherent in periodic cycles, specifically because of parasitoid density and patch-quality effects in the case of the LBM, will tend to resist and delay population responses. Correlation analyses of changes in elevation and temperature were analyzed with 10-y intervals to ensure that the measures from the 10-y moving averages in elevation are independent.

Population Growth Rate–Elevation Relationship. Elevation-specific population growth rate of LBM was estimated by best-fitting simulated LBM population dynamics to empirical time series of larval density. The empirical time series were obtained from 13 sites in the Alps between 500 and 1,950 m asl (13). The tritrophic LBM model (Eqs. **1**–**3**) (31) was simulated across a realistic range of growth rates [$\lambda = 1.1–10.0$ at 0.1 intervals where $r_0 = \ln(\lambda)$]. The cyclical nature of LBM dynamics results in phase-specific rates of population growth. Thus, wavelet-phase analysis was performed on each empirical and simulated time series separately, and the relationships between population growth rate and phase angle were recorded. For each simulation, the growth rate–phase angle relationship was smoothed with a cubic smoothing spline using Matlab 7.4.0. The growth rate at each location was estimated by fitting the empirical data to the appropriate model. The best-fit model to each location was defined as the one with the growth rate that minimized the sum of squares of the difference between empirical and simulated r_0 at the given phase angle (*SI Text*, *Estimating Elevation-Specific Population Growth Rates of LBM* has a graphical example). The functional relationship between elevation and population growth rate was created by best fitting a quadratic curve to the data.

Simulated Spatial Outbreak Dynamics. LBM spatial outbreak patterns were simulated across an elevational gradient using Turchin's tritrophic model of LBM population dynamics (Eqs. **1**–**3**) (31) with the empirically measured effect of elevation on population growth rate. Elevation was scaled from 400 to 2,200 m asl at a resolution of 10 m. Model simulations were performed under two scenarios: constant and fluctuating temperatures. In the former, relative temperature was held constant at multiple values (0 °C, +1 °C, and +2 °C) in the first analysis. For each relative temperature, 10 replicate simulations were run for 560 y at a resolution of one time step per year. The first 500 y of data were discarded before analysis to avoid transient dynamics. The length of the analyzed time series was set at 60 y to be consistent with the three 60-y time intervals in the empirical analysis. Wavelet-phase analysis was used to estimate the time-specific elevation of the outbreak epicenter in simulated time series. The purpose of this exercise was to show (*i*) how a gradient in r_0 can induce elevational traveling waves of outbreak and (*ii*) the predicted positive relationship between temperature and elevation of outbreak epicenters. In a second analysis, the model was simulated at four temperature regimens (0 °C, +1 °C, +2 °C, and +3 °C) to test for a mechanistic effect of climatic warming on damped population cycles and the cessation of LBM outbreaks.

In the fluctuating-temperature model, annual temperature estimates were smoothed with 20-y splines by a previous study (35). For each of the four mean annual seasonal temperatures, the spatial outbreak dynamics were simulated from A.D. 1659 to 2000 and replicated 100 times. Epicenter elevations between A.D. 1800 and 2000 were estimated from simulation data using wavelet-phase analysis and compared with empirical epicenter estimates. The average epicenter elevation for each year is reported for each seasonal temperature regimen.

ACKNOWLEDGMENTS. We thank Eugene Luzader for assistance in preparing Fig. 1. Funding and support were provided by the US Department of Agriculture NRI grant 2006-35306-17264 (to D.M.J.), the Swiss National Science Foundation (NCCR-Climate) (to D.C.F., J.E., and U.B.), and the Centre for Ecological and Evolutionary Synthesis, University of Oslo.

1. Lenoir J, Gégout JC, Marquet PA, de Ruffray P, Brisse H (2008) A significant upward shift in plant species optimum elevation during the 20th century. *Science* 320: 1768–1771.
2. Cleland EE, Chuine I, Menzel A, Mooney HA, Schwartz MD (2007) Shifting plant phenology in response to global change. *Trends Ecol Evol* 22:357–365.
3. Carpenter KE, et al. (2008) One-third of reef-building corals face elevated extinction risk from climate change and local impacts. *Science* 321:560–563.
4. Parmesan C (2006) Ecological and evolutionary responses to recent climate change. *Annu Rev Ecol Evol Syst* 37:637–669.
5. Stireman JO, 3rd, et al. (2005) Climatic unpredictability and parasitism of caterpillars: Implications of global warming. *Proc Natl Acad Sci USA* 102:17384–17387.
6. Sturm M, Racine C, Tape K (2001) Climate change. Increasing shrub abundance in the Arctic. *Nature* 411:546–547.
7. Parmesan C (1996) Climate and species' range. *Nature* 382:765–766.
8. Moritz C, et al. (2008) Impact of a century of climate change on small-mammal communities in Yosemite National Park, USA. *Science* 322:261–264.
9. Parmesan C, Yohe G (2003) A globally coherent fingerprint of climate change impacts across natural systems. *Nature* 421:37–42.

10. Körner C (2007) The use of 'altitude' in ecological research. *Trends Ecol Evol* 22: 569–574.
11. Ims RA, Henden JA, Killengreen ST (2008) Collapsing population cycles. *Trends Ecol Evol* 23:79–86.
12. Kausrud KL, et al. (2008) Linking climate change to lemming cycles. *Nature* 456:93–97.
13. Baltensweiler W, Rubli D (1999) Dispersal: An important driving force of the cyclic population dynamics of the larch bud moth, *Zeiraphera diniana* Gn. *Forest Snow Landscape Res* 74:1–153.
14. Esper J, Büntgen U, Frank DC, Nievergelt D, Liebhold A (2007) 1200 years of regular outbreaks in alpine insects. *Proc Biol Sci* 274:671–679.
15. Johnson DM, Bjørnstad ON, Leibhold AM (2004) Landscape geometry and traveling waves in the larch budmoth. *Ecol Lett* 7:967–974.
16. Bjørnstad ON, Peltonen M, Liebhold AM, Baltensweiler W (2002) Waves of larch budmoth outbreaks in the European alps. *Science* 298:1020–1023.
17. Baltensweiler W, Weber UM, Cherubini P (2008) Tracing the influence of larch-bud-moth insect outbreaks and weather conditions on larch tree-ring growth in Engadine (Switzerland). *Oikos* 117:161–172.
18. Büntgen U, et al. (2009) Three centuries of insect outbreak dispersal across the European Alps. *New Phytol* 182:929–941.
19. Schweingruber FH (1979) Auswirkungen des Lärchenwicklerbefalls auf die Jahrringstruktur der Lärche. *Schweiz Z Forstwes* 130:1071–1093.
20. Weber UM (1997) Dendroecological reconstruction and interpretation of larch budmoth (Zeiraphera diniana) outbreaks in two central Alpine valleys of Switzerland from 1470-1990. *Trees-Structure Function* 11:277–290.
21. Baltensweiler W (1993) Why the larch bud-moth cycle collapsed in the sub-alpine larch-cembran pine forests in the year 1990 for the 1st time since 1850. *Oecologia* 94: 62–66.
22. Carrer M, Urbinati C (2004) Age-dependent tree-ring growth responses to climate in Larix decidua and Pinus cembra. *Ecology* 85:730–740.
23. Körner C (1998) A re-assessment of high elevation treeline positions and their explanation. *Oecologia* 115:445–459.
24. Li M, Yang J, Krauchi N (2003) Growth responses of Picea abies and Larix decidua to elevation in subalpine areas of Tyrol, Austria. *Can J Forest Res—Revue Canadienne De Recherche Forestiere* 33:653–662.
25. Schulze ED, Mischi G, Asche G, Borner A (2007) Land-use history and succession of Larix decidua in the Southern Alps of Italy. An essay based on a cultural history study of Roswitha Asche. *Flora* 202:705–713.
26. Delucchi V (1982) Parasitoids and hyperparasitoids of *Zeiraphera diniana* [Lep. *Tortricidae*] and their role in population-control in outbreak areas. *Entomophaga* 27: 77–92.
27. Benz G (1974) Negative Ruckkopelung durch Raum- und Nahrungskonkkurrenz sowie zyklische Veranderung der Nahrungsgrundlage als Regelsprinzip in der Populationsdynamik des Grauen Larchenwicklers, Zeiraphera diniana (Guenee) (Lep. Tortricidae). *Z Angewandte Entomologie* 76:196–228.
28. Omlin FX (1977) Zur populationsdynamischen Wirkung der durch Raupenfrass und Dungung veranderten Nahrungsbasis auf den Grauen Larchenwickler *Zeiraphera diniana* Gn. (Lep. Torticidae). Doctoral dissertation (Eidgenössiche Technische Hochschule, Zurich).
29. Turchin P, et al. (2003) Dynamical effects of plant quality and parasitism on population cycles of larch budmoth. *Ecology* 84:1207–1214.
30. Hassell MP, May RM (1973) Stability in insect host-parasitoid models. *J Anim Ecol* 42: 693–736.
31. Turchin P (2003) *Complex Population Dynamics: A Theoretical/Empirical Synthesis* (Princeton University Press, Princeton).
32. Nicholson AJ, Bailey VA (1935) The balance of animal populations, part I. *Proc Zool Soc Lond* 105:551–598.
33. Furuta K (1978) *Flight Potential of the Larch Bud Moth, Zeiraphera diniana Gn. (Lep. Tortricidae) on a Flight Mill (Unpublished Report)* (WSL Library, Birmensdorf, Switzerland).
34. National Oceanic and Atmospheric Administration (1976) *U.S. Standard Atmosphere* (Governmental Printing Office, Washington, DC).
35. Casty C, Wanner H, Luterbacher J, Esper J, Bohm R (2005) Temperature and precipitation variability in the European Alps since 1500. *Int J Climatol* 25:1855–1880.
36. Auer I, et al. (2007) HISTALP—historical instrumental climatological surface time series of the Greater Alpine Region. *Int J Climatol* 27:17–46.
37. Büntgen U, Frank DC, Nievergelt D, Esper J (2006) Summer temperature variations in the European Alps, AD 755-2004. *J Clim* 19:5606–5623.
38. Kress A, et al. (2009) Summer temperature dependency of larch budmoth outbreaks revealed by Alpine tree-ring isotope chronologies. *Oecologia* 160:353–365.
39. Day KR (1997) The influence of temperature on egg mortality in the budmoth Zeiraphera diniana (Lepidoptera:Tortricidae), and its role in determining the regional abundance of an important forest pest. *Bull Entomol Res* 87:259–264.
40. Chauchard S, Beilhe F, Denis N, Carcaillet C (2010) An increase in the upper tree-limit of silver fir (Abies alba Mill.) in the Alps since the mid-20th century: A land-use change phenomenon. *For Ecol Manage* 259:1406–1415.
41. Harsch MA, Hulme PE, McGlone MS, Duncan RP (2009) Are treelines advancing? A global meta-analysis of treeline response to climate warming. *Ecol Lett* 12:1040–1049.
42. Moser B, Temperli C, Schneiter G, Wohlgemuth T (2010) Potential shift in tree species composition after interaction of fire and drought in the Central Alps. *Eur J For Res* 129:625–633.
43. Luterbacher J, et al. (2007) Exceptional European warmth of autumn 2006 and winter 2007: Historical context, the underlying dynamics, and its phenological impacts. *Geophys Res Lett* 34:L12704.
44. Stott PA, Stone DA, Allen MR (2004) Human contribution to the European heatwave of 2003. *Nature* 432:610–614.
45. Intergovernmental Panel on Climate Change (2007) *Climate Change 2007: The Physical Science Basis. Contribution of Working Group I to the Fourth Assessment Report of the Intergovernmental Panel on Climate Change* (Cambridge University Press, Cambridge, UK).
46. Logan JA, Regniere J, Powell JA (2003) Assessing the impacts of global warming on forest pest dynamics. *Front Ecol Environ* 1:130–137.
47. Buntgen U, Frank D, Wilson R, Carrer M, Urbinati C (2008) Testing for tree-ring divergence in the European Alps. *Glob Change Biol* 14:2443–2453.